Microstructures and mechanical property of a Fe-Ni-Al-C alloy containing B2 intermetallic compounds

Si Gao[*, 1], Yu Bai[1,2], Akinobu Shibata[1,2], Nobuhiro Tsuji[1,2]

[1]Department of Materials Science and Engineering, Kyoto University, Sakyo-ku, Kyoto, 606-8501, Japan
[2]Elements Strategy Initiative for Structural Materials (ESISM), Kyoto University, Yoshida Honmachi, Sakyo-ku, Kyoto 606-8501, Japan

[1]E-mail address: gao.si.8x@kyoto-u.ac.jp

Keywords: high strength steel, intermetallic compounds, mechanical property
Abstract. Specimens of a Fe-24Ni-6Al-0.4C alloy with ultra-fine grained dual phase microstructures composed of FCC austenite and B2 phases were fabricated by cold rolling followed by annealing treatments in the temperature range from 850°C to 1100°C. Tensile tests of these specimens revealed a similar yield stress while the tensile strength was found to vary significantly. The different tensile strength of the samples was considered to be caused by the different volume fractions of the hard B2 phase.

1. Introduction

It is well-known that intermetallic compounds are usually avoided in designing metallic alloys because their brittleness leads to poor ductility of the whole material [1]. However, recently some research has shown that some alloys containing intermetallic compounds as relatively coarse second-phase particles can exhibit a good combination of strength and tensile ductility [2-4]. It is believed that the intermetallic compound plays an important role in such superior mechanical properties of these materials, but the detailed mechanisms responsible for this have not yet been studied and clarified. In the present study, the microstructure and tensile behavior of a Fe-24Ni-6Al-0.4C alloy, containing a NiAl-type B2 intermetallic compound, were investigated in order to understand the mechanism responsible for good mechanical properties in this new type of alloy.

2. Experimental procedures

An alloy having a chemical composition of Fe-24Ni-6Al-0.4C (mass%) was used in the present study. An as-received thick plate of 10 mm in thickness was homogenized at 1280°C for 5 hours in argon atmosphere, quenched into water, and then cold rolled to 1.15 mm in thickness, corresponding to an 88.5% rolling reduction. In order to obtain different microstructures, the cold-rolled sheets were annealed at different temperatures ranging from 850°C to 1100°C for 10 minutes using either a salt bath or a vacuum furnace and then quenched into water. Tensile test specimens of 10 mm in gauge length, 5 mm in gauge width and 1 mm in thickness were cut from the as-homogenized plate or from the cold rolled and subsequently annealed sheets using electron discharge machining. The tensile tests were carried out at room temperature at an initial strain

rate of 8.3×10^{-4} s^{-1}. Prior to tensile testing the surface of each specimens was covered by white paint and then by a dispersion of black spots, in order to conduct digital image correlation (DIC) analysis. Images were taken during tensile testing by a CCD camera and then analyzed using the VIC2D software allowing a precisely measurement of both the tensile elongation and the strain distribution in the specimen during tensile deformation.

Microstructures of the specimens were observed in a scanning electron microscope (SEM) using back-scattered electron (BSE) contrast, and by electron back-scatter diffraction (EBSD) on longitudinal sections taken perpendicular to the transverse direction (TD) of the sheets. Average grain sizes of the specimens were determined by the linear intercept method from EBSD grain boundary maps.

3. Results and discussion

An EBSD grain boundary map and phase map of the as-homogenized specimen are shown in figure 1, which reveals an almost single austenitic (FCC) phase, fully recrystallized microstructure having a very coarse grain size around 150 µm. Some small B2 particles can be observed on grain boundaries of the austenite matrix, although the fraction of this phase is very small.

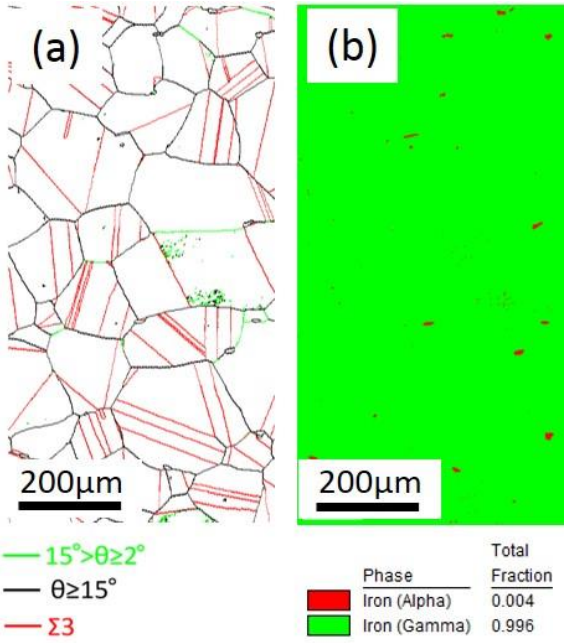

Figure 1. EBSD boundary map (a) and phase map (b) of the as-homogenized specimen. Low angle grain boundaries, high angle grain boundaries and twin boundaries are denoted by green, black and red colors, respectively in (a). The austenite phase (gamma) and B2 phase (recognized as alpha phase) are denoted by green and red colors in (b).

Example microstructures of the cold rolled and subsequently annealed specimens are shown in figure 2. Austenite and B2 phases can be easily distinguished from their dark and white contrast from the SEM-BSE images. It is seen in figure 2 (a) that the specimen annealed at 850°C has a fully recrystallized dual phase microstructure, characterized by equiaxed grains of the austenite phase with very fine grain sizes, and B2 particles that are mostly dispersed on grain boundaries and triple junctions of the austenite phase. From the EBSD observations, the measured average

grain size of the austenite matrix was determined as 0.45 μm. The area fraction and average grain size of the B2 phase in this specimen were 61.8% and 0.17 μm, respectively. With increasing annealing temperature up to 1000°C, the area fraction of the B2 phase greatly decreased to 35%, accompanied by an overall microstructural coarsening, as seen figure 2(b). At 1000 °C the average grain sizes of the austenite matrix and B2 phase were increased to 0.32 μm and 0.7 μm, respectively. With further increase of annealing temperature to 1100°C, the area fraction of the B2 phase decreased to 16.6%, accompanied by a slight increase in the average grain size of austenite matrix and B2 phase to 0.37 μm and 1.1 μm, respectively. It should be noted that the material maintained an ultrafine-grained microstructure at elevated temperatures as high as 1100°C, which has been scarcely observed in conventional single or dual phase alloys [5-7]. The stability of the ultrafine microstructure is probably because the B2 phase does not dissolve even at high temperature, owing to the excellent thermal stability of such intermetallic compounds. As such The B2 particles dispersed on grain boundaries and triple junctions greatly inhibited the grain growth of the FCC (austenite) matrix by exerting a dragging force on migrating grain boundaries, thus allowing ultrafine grained microstructures to be maintained even after annealing at high temperatures [8].

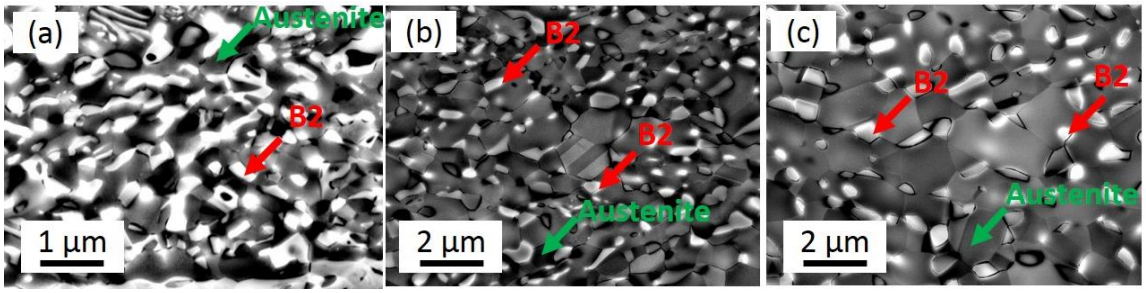

Figure 2. Microstructures of the cold-rolled and subsequently annealed specimens observed by SEM-BSE; (a) 850°C for 10 minutes, (b)1000°C for 10 minutes and (c) 1100°C for 10 minutes. Austenite (FCC) matrix in dark contrast and B2 phase in bright contrast are pointed out by green and red arrows, respectively. A decrease in the amount of B2 phase with increasing the annealing temperature can be readily observed.

Example tensile stress-strain curves of the as-homogenized, and the cold rolled and subsequent annealed specimens are shown in figure 3. The yield stress, tensile strength and total elongation of the as-homogenized specimen were 226 MPa, 600 MPa and 23%, respectively. After 88.5% cold rolling, the specimen showed a dramatically increased yield strength and tensile strength of 1543 MPa and 1770 MPa, respectively, but a quite limited total elongation of only 3%. Such tensile properties have often observed in heavily deformed austenitic steel, due to the highly deformed microstructures and associated low strain hardening capability [9,10]. On the other hand, it is noteworthy that the cold rolled and subsequently annealed specimens exhibited quite different tensile properties depending on the annealing temperature. The 850°C annealed specimen showed a significantly reduced yield strength of 558 MPa but an even higher tensile strength of 1923 MPa and a restored tensile elongation of 10%, compared with those of the cold rolled specimen. With increasing the annealing temperature to 1000°C and 1100°C, the tensile strength decreased to 1618 MPa and 1124 MPa, with the total elongation gradually increasing to 18% and 21%, respectively. It should be emphasized that although the annealed specimens having ultrafine grain microstructures and B2 particles exhibited moderate yield strength and total elongation, they showed significant larger strain hardening and ultimate tensile strengths, compared with other ultrafine grain materials having single austenite phase [6,7].

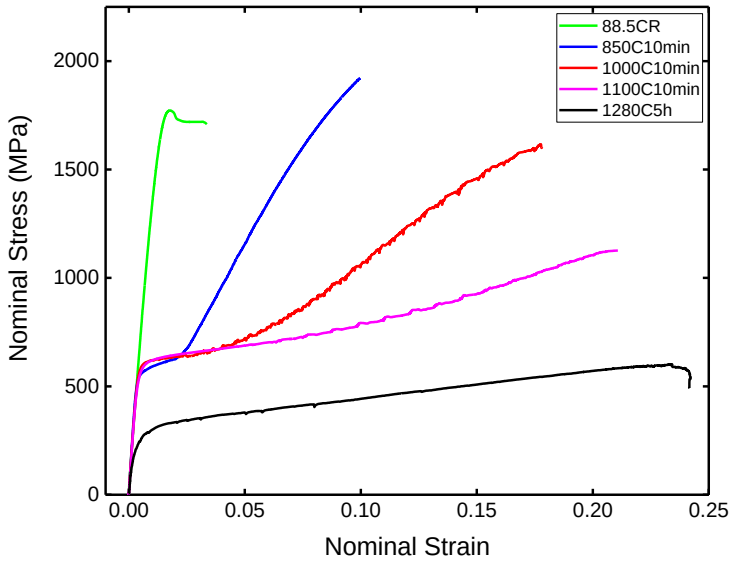

Figure 3. Nominal stress-strain curves of the as-homogenized(1280°C for 5 hours), 88.5% cold rolled, cold rolled and subsequently annealed Fe-24Ni-6Al-0.4C specimens.

Serrated flow can be clearly observed on stress-strain curves of the 1000°C and 1100°C annealed specimens, which indicates the occurrence of the deformation induced martensitic transformation that is often observed in Fe-Ni-C alloy systems [11]. It is very interesting that the annealed specimens have an approximately identical value of the yield strength (~600 MPa) and exhibit similar deformation behavior at early stage of tensile deformation. More specifically, the stress-strain curves of the annealed specimens exhibited a smooth transition from elastic deformation to plastic deformation (continuous yielding), followed by a nearly plateau-like part with a low strain hardening rate, which continued to about 2.5% plastic strain. After this plateau, the specimens showed pronounced differences in strain hardening and eventually fractured without necking, indicating an early fracture before plastic instability. Using the digital image correlation analysis, it was confirmed that the plateau-like flow curve corresponded to the formation and propagation of localized deformation bands, similar to Lüders-band deformation characteristic after discontinuous yielding in carbon steels (results to be published in another paper). Discontinuous yielding has been well-known to occur in low carbon ferritic steels due to a strong interaction between interstitial atoms (carbon and nitrogen) and dislocations. Moreover, it has been found recent years that discontinuous yielding is an universal mechanical behavior in most metallic materials with ultrafine grain sizes [12], although the mechanism of the interesting phenomena in UFG metals is still not fully understood. Considering the fine grain sizes and high carbon content of the specimens used in the present study, it is not surprising to observe discontinuous yielding and a low strain hardening rate at early stages of the tensile tests. However, discontinuous yielding phenomena are generally characterized by a distinct yield drop at the elasto-plastic transition, which is not observed in the present material. It is considered that the absence of the distinct yield drop and the plateau-like portion at the early stage of the tensile test in the present material is due to the exceptionally high strain hardening rate, which can partially compensate the stress drop during yielding, resulting in only the plateau flow in the beginning of tensile deformation.

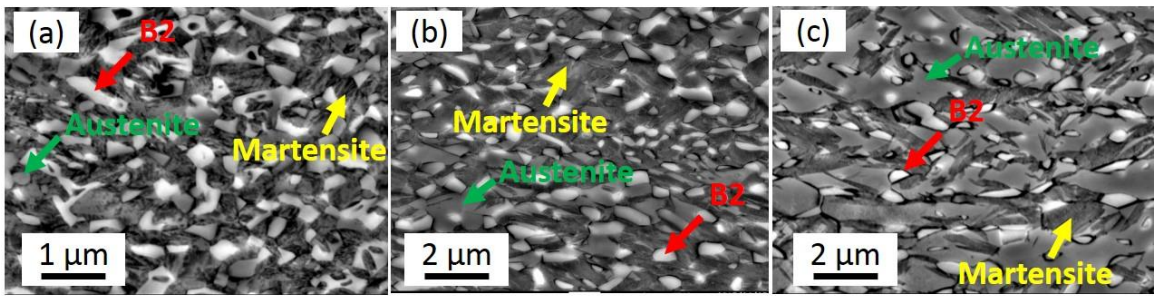

Figure 4. SEM micrographs of (a) 850°C annealed, (b) 1000°C annealed and (c) 1100°C annealed specimens after tensile fracture. The austenite phase, B2 phase and deformation induced martensite phase are denoted by green, red and yellow arrows, respectively.

After the early plastic strain stage with low strain hardening rate, the stress strain curves start to exhibit higher strain hardening rates. To explain the large difference in the strain hardening behavior of the present material containing B2 phase, microstructures of the annealed specimens after tensile deformation were observed and are shown in figure 4. Martensite phase can be clearly distinguished by the dark contrast on the micrographs of all three specimens, indicating that deformation induced martensitic transformation occurred during the tensile tests. It is seen that after the tensile deformation, a large fraction of austenite still remained in the 1100°C annealed specimen while only smaller amounts of austenite remain in the 1000°C and 850°C annealed specimens. The area fractions of martensite after the tensile deformation were also quantitatively measured by EBSD. Since EBSD mapping analysis cannot distinguish BCC martensite and B2 phases, the area fraction of martensite was calculated as the difference of the BCC phases before and after tensile deformation.

Table 1. Phase fractions of austenite, B2, and martensite measured by SEM-EBSD before and after tensile deformation.

Specimen	Phase fraction before tensile test (%)		Phase fraction after tensile test (%)		
	Austenite	B2	Austenite	B2	Martensite
850°C10min	38.1	61.8	7.6	61.8	30.6
1000°C10min	64	35.5	34.7	35.5	29.3
1100°C10min	83.4	16.6	51.3	16.6	32.1

The area fraction of each phase before and after tensile testing is summarized in table 1. Here it was assumed that the fraction of B2 phase did not change by the deformation. It should be noted that the fraction of the deformation induced martensite after tensile deformation was almost the same, approximately 30% in all the three specimens, although the initial area fraction of austenite was quite different depending on the annealing temperature. Thus the differences in the phase fraction among these three specimens after the tensile deformation mainly came from the amount of B2 phase and remaining austenite. It is well known that austenite is much softer than martensite or B2 phases that have a BCC or ordered BCC crystal structure, thus the contribution of the remaining deformed austenite to the overall tensile strength is considered to be small. Considering that the fraction of martensite is nearly identical in all of the three specimens, while B2 phase fraction is quite different, the large difference in the ultimate tensile strength is likely to

arise from the different fraction of the B2 phase in each specimen. In other words, the large area fraction of B2 in the 850°C annealed specimen contributes predominantly to its high strain hardening and high tensile strength. As the area fraction of the B2 phase decreases with increasing the annealing temperature, the strain hardening and tensile strength of the specimens also decrease with increasing annealing temperature.

4. Conclusion

1. Fe-24Ni-6Al-0.4C alloy specimens having ultrafine grained and dual-phase microstructures composed of a FCC matrix and B2 phase were fabricated by cold rolling followed by subsequent annealing. The amount of B2 phase decreased from 61.8% to 16.6% by increasing the annealing temperature from 850°C to 1100°C. The dispersed B2 particles greatly impeded the microstructure coarsening process during annealing, allowing an ultrafine grained FCC matrix to be maintained even after annealing at 1100°C.
2. Tensile tests revealed a moderate strength and total elongation in the as-homogenized specimen having a coarse-grained microstructure, but very high strain hardening and ultimate tensile strengths in the ultrafine grained specimens containing B2 phase.
3. EBSD investigations revealed that the amount of deformation-induced martensite was almost same in all the annealed specimens. It was considered therefore that the volume fraction of B2 phase plays an important role in the strain hardening behavior and high tensile strength of the UFG specimens annealed at different temperatures.

Acknowledgments

This work was financially supported by the Elements Strategy Initiative for Structural Materials (ESISM), and the Grant-in-Aid for Scientific Research (S) (No. 15H05767), all through the Ministry of Education, Culture, Sports, Science and Technology(MEXT), Japan.

References

[1] Deevi S C and Sikka V K 1996 *Intermetallics* **4** 357–375
[2] Furuta T, Kuramoto S, Ohsuna T, Oh-Ishi K and Horibuchi K 2015 *Scr. Mater.* **101** 87–90
[3] Kim S H, Kim H and Kim N J 2015 *Nature* **518** 77–79
[4] Yang M X et al. 2016 *Acta Mater.* **109** 213–222
[5] Sun G S et al. 2015 *Mater. Charact.* **110** 228–235
[6] Dini G, Najafizadeh A, Ueji R and Monir-Vaghefi S M 2010 *Mater. Des*. **31** 3395–3402
[7] Tian Y Z et al. 2017 *Mater. Charact.* **126** 74–80
[8] Munoz-Morris M A, Calderon N and Morris D G 2008 *J. Mater. Sci.* **43** 3674–3682
[9] Miura H et al. 2017 *Scr. Mater.* **133** 33–36
[10] Ondobokova M, Belyakov A, Enikeed N, Molodov D A and Kaibyshev R 2017 *Mater. Sci. Eng.* A **689** 370–383
[11] Suh D W, Park S J, Lee C H and Kim S 2009 *J. Metall. Mater. Trans. A Phys. Metall. Mater. Sci.* **40** 264–268
[12] Tsuji N, Ito Y, Saito Y and Minamino 2002 *Scr. Mater.* **47** 893–899